

# Stress Distribution Patterns within Viscero- and Neurocranium during Nasoalveolar Molding: a Finite Element Analysis

Lucas M. Ritschl, MD, DMD\*

Veronika Heinrich, MSc†

Florian D. Grill, MD\*

Maximilian Roth, MD\*‡

Dennis M. Hedderich, MD§

Andrea Rau, MD, DDS, PhD\*

Klaus-Dietrich Wolff, MD, DDS,

PhD\*

Franz X. Bauer, MSc†

Denys J. Loeffelbein, MD, DDS,

PhD\*‡

**Background:** The purpose of this study was to evaluate the stress distribution patterns within the viscer- and neurocranium of neonates during nasoalveolar molding.

**Methods:** Finite element models of 3 different healthy neonates at different times of life (date of birth, 4 weeks, and 3.5 months) were generated on the basis of computed tomography scans. A validated workflow, including segmentation, meshing, setting of boundary conditions, and implementation of a bone density-dependent material model, was carried out for each model. A small and a large unilateral alveolar and hard palatal cleft were virtually cut in each model. The stress distribution pattern in each model was then analyzed by using Ansys APDL.

**Results:** Convergence analysis validated the results. The virtual experiments at the date of birth showed a stress pattern above a previously defined threshold value of 30,000 Pa in the ipsilateral naso-orbital-complex, frontal sinus, and the anterior fossa of the base of the skull, with von Mises values > 35,000 Pa. Stress patterns at the age of 4 weeks and 3.5 months showed reduced von Mises values at < 15,000 Pa.

**Conclusions:** Nasoalveolar molding therapy is a safe presurgical treatment modality without significant influence on the viscer- and neurocranium of neonates. Treatment, considering the stress distribution at the naso-orbital-complex and anterior fossa of the base of the skull, should begin in the second week of life, and treatment initiation of preterm infants should be adapted respectively. (*Plast Reconstr Surg Glob Open* 2018;6:e1832; doi: 10.1097/GOX.0000000000001832; Published online 17 July 2018.)

## INTRODUCTION

Nasoalveolar molding (NAM) has been shown to influence positively the treatment of patients affected with

cleft lip and palate (CLP) following its introduction by Grayson et al.<sup>1</sup> Initially, a simplified narrowing of the alveolar gap and the cleft lip width and a significant prolongation of the columella, especially in bilateral CLP cases, was reported.<sup>2,3</sup> Evidence-based long-term results are still lacking, but a trend toward the reduction of secondary corrections has been correlated positively with this presurgical treatment, because of less scarring and improved nasal symmetry.<sup>4-7</sup> Recently, computer-aided design and computer-aided manufacturing techniques have been introduced to the treatment algorithm of NAM therapy.<sup>8-10</sup> In this context, the integration shows a reduced need of imprint-taking with comparable clinical results, possibly further optimizing the patient's and parent's compliance, 1 of the main difficulties associated with this treatment modality.<sup>11</sup>

The advantageous and disadvantageous effects of NAM and other presurgical orthopedics remain the subject of controversy.<sup>12-15</sup> Although a positive effect on the treatment course has been reported, stress distribution patterns on the viscer- and neurocranium and evidence-

*From the \*Department of Oral and Maxillofacial Surgery, Klinikum rechts der Isar, Technische Universität München, Germany; †Institute of Medical and Polymer Engineering, Technische Universität München, Germany; ‡Department of Oral and Maxillofacial Surgery, Helios Hospital Munich West, Teaching Hospital of Ludwig-Maximilians-Universität München, Germany; and §Department of Neuroradiology, Klinikum rechts der Isar, Technische Universität München, Germany. Received for publication March 29, 2018; accepted April 18, 2018.*

*The project RapidNAM for digitalization and automatization of NAM therapy is financially supported by the Zeidler-Forschungs-Stiftung (Waldkraiburg, Germany).*

*Mr. Bauer and Dr. Loeffelbein contributed equally to this work.*

*Copyright © 2018 The Authors. Published by Wolters Kluwer Health, Inc. on behalf of The American Society of Plastic Surgeons. This is an open-access article distributed under the terms of the Creative Commons Attribution-Non Commercial-No Derivatives License 4.0 (CCBY-NC-ND), where it is permissible to download and share the work provided it is properly cited. The work cannot be changed in any way or used commercially without permission from the journal.*

DOI: 10.1097/GOX.0000000000001832

**Disclosure:** The authors have no financial interest to declare in relation to the content of this article. The Article Processing Charge was paid for by the authors.

based long-term effectiveness caused by the various treatment modalities are still lacking. Finite element analysis (FEA) has been shown to be a valid and reproducible method for analyzing resulting stress distribution patterns<sup>16</sup> and has been applied, for example, in orthodontic, orthognathic surgery, and traumatological studies involving the head and face region.<sup>17–22</sup> Nevertheless, no valid finite element (FE) models with the corresponding material properties of neonate tissue (bone, cartilage, and soft tissue) are available. In previously reported cases of FEA in children by others, the mean age of the virtual skulls of most studies was significantly older than the age or time interval when neonates are treated with NAM therapy,<sup>23–25</sup> because treatment is performed during the first 12–16 weeks of life.

The purpose of this study was to establish a simplified FE model, based on assumption described in the literature. Further, we wanted to analyze the resulting forces and stress distribution patterns in neonates at 3 different time points during the presurgical treatment interval of NAM therapy. The FE models were set up as worst-case scenarios to determine the largest influence that NAM therapy could provoke.

## MATERIALS AND METHODS

### Ethical Statement and Patient Recruitment

All investigations and procedures were conducted according to the principles expressed in the Declaration of Helsinki. An exemption from the requirement of ethics approval was granted by the Ethical Committees of the Technische Universität München and of the Universität zu Köln because of anonymized evaluation of previously existing computed tomography (CT) scans and an initial willingness of the patients to undergo the required medical procedures (Approval No. 392/15 and 15–329). The enrolment criterion for the CT scan was a normal development of the viscerocranium and neurocranium. The initial indications for the CT scans were exclusion of choanal atresia (date of birth), intracranial bleeding (at 4 weeks of life), and subsequent traumatic brain injury (at 3.5 months of life).

### Construction of the Finite Element Models

A common protocol of FE model generation was used as previously described.<sup>26</sup> In summary, DICOM data sets of 3 CT scans were segmented in MIMICS (MIMICS 16.0, Materialise; Leuven, Belgium) to export 3-dimensional (3D) models (Table 1). The available CT scans of 3 healthy neonates were taken at 3 different time stages adapted to the conventional initiation and treatment duration of presurgical period of NAM therapy: at date of birth, at 4 weeks, and at 3.5 months of age. On the basis of the 3D models of the healthy neonates (= original CT scan), 2 additional models each were virtually created, 1 with a small (~ 4.5 mm width) and 1 with a large (~ 12 mm width) cleft of the alveolar crest and hard palate in the models at 4 weeks and 3.5 months of age. In the newborn model, only a small cleft was simulated. Subsequently, the

**Table 1. Resolution of CT Scans Varied between Patients**

Modality	Information	0 d	4 wk	3.5 mo
CT scan	Layer distance (mm)	0.5	1.5	0.5
	Amount of layers (-)	103	106	254
	Pixel size (mm)	0.205	0.320	0.430
Mesh	Element size (mm)	0.25–0.5	0.25–1.5	0.25–1.5
	Nodes (-)	1,200,000	900,000	1,400,000

The element size resolution was adapted to the area for the 4 weeks and 3.5-month-old patient (anterior skull: 0.5–0.75, posterior skull 0.75–1.5, region of force application 0.25–0.5).

3D models were exported to 3-MATIC (3-MATIC 8.0, Materialise; Leuven, Belgium) and smoothed, the area of applied forces was defined for each model separately and the applicable models were then meshed in ANSYS ICEM CFD (ANSYS 16.0, ANSYS Inc.; Pa.; Table 1). The virtual mesh of each model was again imported to MIMICS, and the bone density-dependent material properties were allocated. Finally, the 3D geometries were exported to ANSYS APDL (ANSYS APDL 16.0, ANSYS Inc.; Pa.) for FEA (Fig. 1).

### Material Property and Simulation Model

The material behavior of cranial bone was defined as an isotropic linear-elastic model with age-dependent material properties. For the establishment of an age-matched corresponding elastic modulus (E-modulus) of the cranial bone, we inter- and extrapolated previously published data from McPherson and Kriwall.<sup>27</sup> The calculated E-modulus ranged from 1,337 to 3,367 MPa for the newborn (date of birth), from 1,737 to 3,767 MPa for the 4-week-old infant, and from 2,738 to 4,768 MPa for the 3.5-month-old infant at a Poisson ratio of 0.28, respectively (Fig. 2). As previously reported, the germs of teeth with the partial beginning of mineralization only influence the results to an extremely limited amount. Thus, the teeth germs were modeled as empty space emphasizing the worst-case scenario, because the empty space simulation resulted in slightly larger stresses than the filled teeth germ simulations.<sup>26</sup> A stress of 30,000 Pa was determined as the critical threshold value for resulting deformation over time as seen in positional plagiocephaly, as previously described.<sup>26,28,29</sup>

All supporting reactions were constrained to 0 with Dirichlet boundary conditions at the bitemporal level of the virtual skull. We applied a force of 0.7 N representing an ulceration force derived by a spring scale with a 3 mm<sup>2</sup> cross-section at the vestibular region of the canines on both sides over an area of 40–60 mm<sup>2</sup>, representing the actual contact area between the NAM plate and the maxilla. The applied force of 0.7 N represents an ulceration force that causes local ischemia of the oral mucosa in a small case series of healthy adults (data not published). In cases a NAM plate causes ulceration, the plate is immediately adapted. Thus, the assumption of a long-term ulceration force in our simulation emphasizes the worst-case character of our study. Furthermore, we did not segment the open sutures to have a direct unphysiological force conduction neglecting dampening effects of the soft tissue.

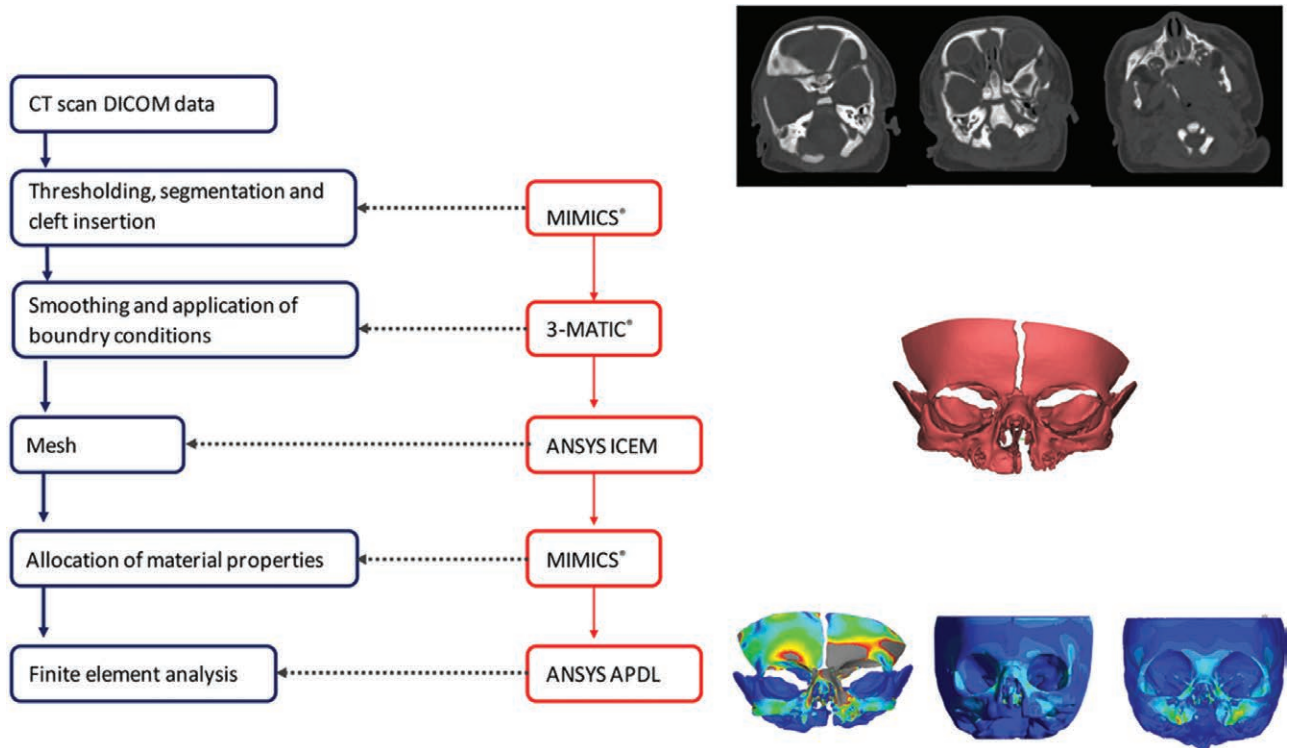


**Fig. 1.** Workflow for FE model generation on the basis of preexisting CT scans by using MIMICS, 3-MATIC, and ANSYS ICEM and ANSYS APDL.

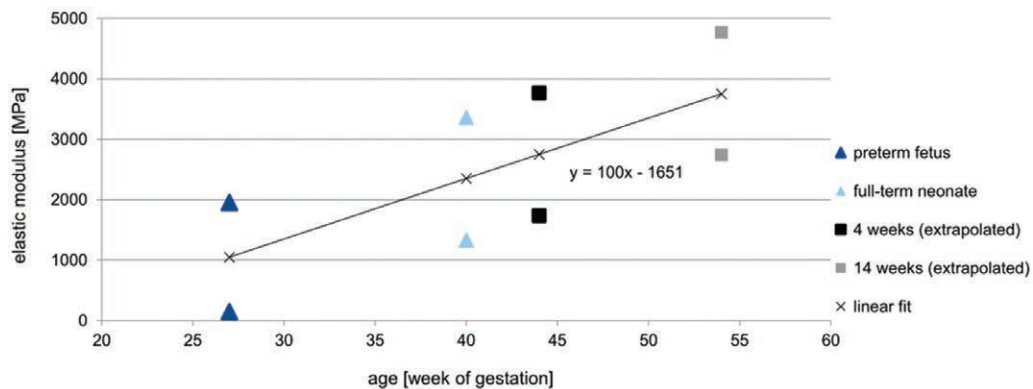


**Fig. 2.** Expected material behavior of cranial bone according to an isotropic linear-elastic elastic model with age-dependent material properties. For establishment of an age-matched corresponding elastic modulus (E-modulus) of the cranial bone, previously published data by McPherson and Kriwall<sup>27</sup> were inter- and extrapolated.

## RESULTS

For all simulated 5 cleft situations, the increased stresses occurred in the same characteristic areas: at the maxilla, vomer, and ossis nasale, lacrimale, ethmoidale, and frontale. In the model of the date of birth, the ossis parietale, temporale, and sphenoidale and the anterior fossa of the base of the skull were additionally involved. At the date of birth, von Mises stress distribution exceeded the previously defined threshold of 30,000 Pa, especially in the ipsilateral naso-orbito-ethmoidal complex, frontal sinus, and the anterior fossa of the base of the skull (Figs. 3, 4). The CT scan of the newborn showed finer osseous structures than the scans of the 4-week-old and 3.5-month-old

neonates. The finest structures of the newborn lay within a single pixel diameter (0.32 mm; Fig. 3), whereas for the 4-week-old and 3.5-month-old neonates, the scans did not show such small structures and thus such peak stresses. The force flux ran via the palate from 1 force application area to the opposite area in the simulations of the healthy skulls.

The width of the cleft gap qualitatively influenced neither the force flux nor the occurring peak stresses.

A quantitative comparison was derived within 4 planes in the area of the viscerocranium (planes A–D) and the anterior and middle fossa of the base of the skull (planes E–H) by calculating the arithmetic mean stress for each



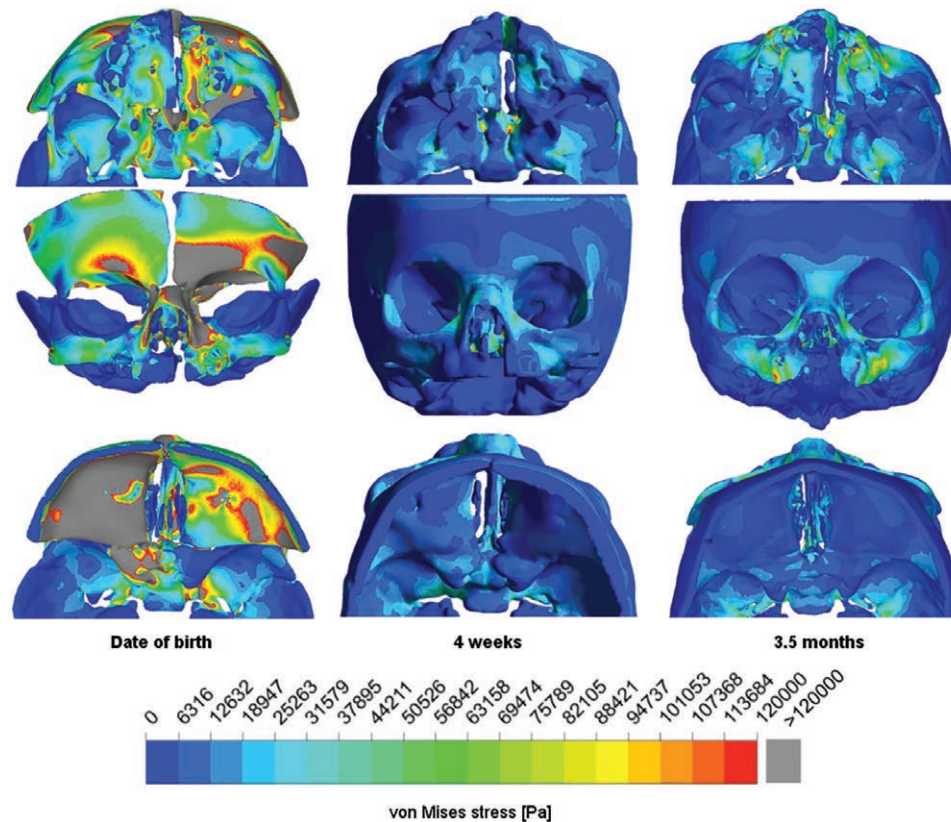


**Fig. 3.** Von Mises stress distribution for the simulated skull in the caudal (upper row), coronar (middle row), and cranial (lower row) view of the newborn (left column), 4-week-old (middle column), and 3.5-month-old (right column) neonates.

plane of each simulation (Fig. 4). The resulting stress values were compared with the threshold value derived from a plagiocephaly case to validate the simulation in each plane and to detect any stress patterns that might cause deformations. The arithmetic means for the 4-week-old and 3.5-month-old neonates remained below the von Mises threshold value of 30,000 Pa and within a range of 15,000 Pa or less for von Mises stress, whereas the von Mises stress for the newborn reached 3 times the threshold von Mises stress value of 30,000 Pa.

The global von Mises peak stress is shown in Table 2 by the 99.9th percentile to avoid having to consider peak stresses attributable to unrealistic small structures.

## DISCUSSION

Several studies of the last few decades have described the typical facial growth and appearance of patients presenting with CLP, based on radiological and clinical follow-up examinations.<sup>25,30,31</sup> A standardized comparison of reported results is nearly impossible because of the wide heterogeneity of treatment algorithms and applied techniques and the lack of controlled randomized trials. Furthermore, and as stated earlier by Berkowitz,<sup>13</sup> “all clefts cannot be lumped together as a single phenomenon.” Various preoperative orthofacial treatments have been described to affect the growing alveolar crest, max-

illa, and nose positively with regard to growth, symmetry, and function.<sup>32</sup> In particular, NAM therapy has been shown to be a valuable treatment, and the first reported long-term analyses have revealed that it might significantly reduce secondary corrections.<sup>4,6</sup> On the other hand, NAM has also been criticized because of its unknown effectiveness or because of unrecognized significant clinical differences between infants with or without treatment by NAM, especially with regard to facial growth and symmetry, maxillary arch dimension, and occlusion.<sup>6,12,13,32–35</sup> It is described that disrupting the premaxillary-vomerine suture may cause severe midfacial retrusion.<sup>36</sup> Disruption may be a result of operative (eg, operative premaxillary setback) or inappropriate presurgical procedures (Latham apparatus or NAM) and needs maxillary advancement in follow-up.<sup>15,37,38</sup> The forces and distribution of stress patterns that might evolve within the viscerocranium and neurocranium during NAM therapy are unknown. Interestingly, no simulations have been performed with regard to force distribution and possible impact (sutural hematoma and impairment of growth) on that sensitive region in case of exceeding forces. Only some clinical, retrospective analyses exist. Lee et al.<sup>39</sup> have assessed the effects of NAM therapy with or without gingivoperiosteoplasty in 20 patients presenting with Unilateral Cleft Lip and Palate (UCLP) by analyzing lateral cephalograms at 6 years and 11.5 years of age. They have reported that midface growth in sagittal or

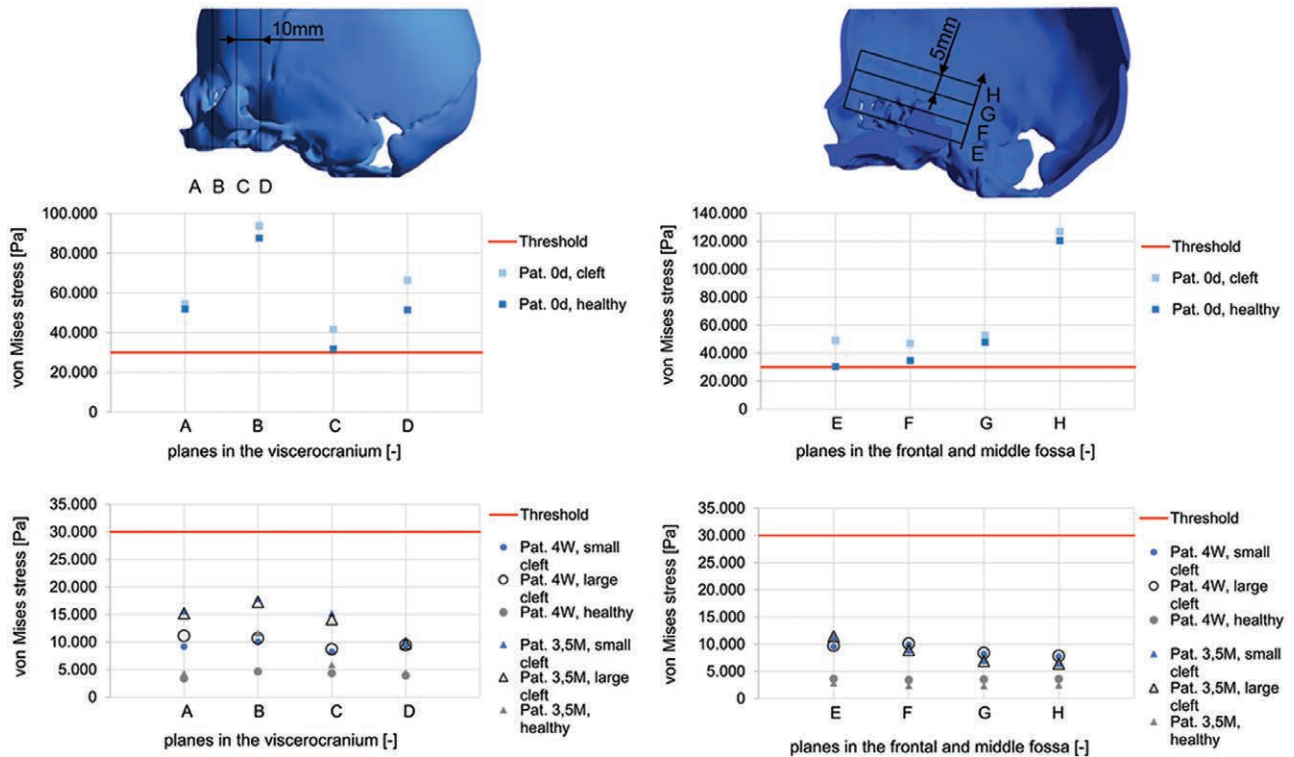


**Fig. 4.** Quantitative comparison of median of von Mises stress in the viscerocranium (planes A–D) and the neurocranium (planes E–H) for the healthy skulls and the simulated cleft situations with variable cleft width. The resulting stress values were compared with the threshold value.<sup>26</sup> The arithmetic means for the 4-week-old and 3.5-month-old neonates remained below the von Mises threshold value of 30,000 Pa and within a range of 15,000 Pa or less for von Mises stress, whereas the von Mises stress for the newborn reached 3 times the threshold von Mises stress value of 30,000 Pa.

**Table 2. Global Peak von Mises stress [Pa] for the 8 Finite Element Models at Date of Birth, 4 Weeks, and 3.5 Months of Age of Model (Healthy, Small, and Large Cleft)**

Model	Date of Birth	4 wk	3.5 mo
Healthy	720,000	33,000	96,000
Small cleft	857,000	57,000	108,000
Large cleft	—	59,000	118,000

The peak stress was determined as the 99.9th percentile.

vertical planes is not affected by presurgical alveolar molding. Other studies have concentrated on the analysis of the nasal symmetry of presurgically treated children with CLP.<sup>40</sup> However, the results based on photographs and X-rays show no force distribution, especially in the regions of the naso-orbito-ethmoidal complex, frontal sinus, and the anterior fossa of the base of the skull.

FEA is a suitable method for simulations and for providing clinical observations and therapies with reproducible analyses. Nevertheless, FEA involving fetal cranial bone and with special regard to growth and the effect of various therapeutic modalities in neonates are lacking. On the 1 hand, fetal cranial bone is a thin, curved, and inhomogeneous material. For this reason, its mechanical properties are difficult to determine. Furthermore, fetal or newborn cranial bone is rarely biomechanically examined, because of ethical reasons. The mechanical properties reported in the literature are therefore also heterogeneous.<sup>41–45</sup>

We decided to use the mechanical properties reported by McPherson and Kriwall,<sup>27</sup> because of their systematic analyses of fetal cranial bone, which seemed conclusive and valid. Furthermore, their results allowed us an extrapolation based on the common assumption that the mechanical properties change according to an isotropic linear-elastic model. According to the literature, it is not clearly defined whether a linear-elastic or plastic model would have been the right to choose. Gačnik et al.<sup>46</sup> described a linear-elastic behavior of the mandibular bone if the strain was within 1–2%. Jiang et al.<sup>47</sup> used also a linear-elastic constitutive model to simulate the skull and sutures in their analysis of fracture characteristics in infant skulls. An accurate modeling of biological tissues requires the experimental characterization of the inhomogeneous structures.<sup>48</sup> Simulations, established to describe the inhomogeneous facial structures, are also based on numerous assumptions [Roth 2010]. For that reason, our presented FE model and analysis represent a worst-case scenario. We did not segment the sutures of the viscerocranium and neurocranium as reported by others,<sup>44</sup> and we applied a force (0.7N) that would result in mucogingival ulceration, if it was not corrected immediately.<sup>49</sup> Therefore, our results from the stress distribution patterns are expected to be higher than those in vivo. In particular, in the case of the scan of the newborn, a lower stress distribution can be expected, because such small structures (0.32mm) as observed in the model are in reality supported by sur-

rounding tissue, which would partially absorb or transmit the incoming load state. The reason for the small structures in the scan of the newborn can also be explained by the resolution of the scan, which had a third of the layer thickness compared with the other scans. A higher layer resolution leads to finer osseous structures, resulting in increased peak stress because the occurring force needs to pass these fine structures.

Our results show increased von Mises values exceeding the previously defined threshold (30,000 Pa) along the expected force flux. Exceeding peak values were registered in the regions of the ipsilateral naso-orbito-ethmoidal complex, frontal sinus, and the anterior fossa of the base of the skull. This result has to be kept in mind when it comes to the timing and initiation of NAM therapy. For this reason, we have corrected the time at which we start our NAM therapy to the second week of life, in contrast to an earlier study.<sup>2</sup> Furthermore, we now adapt the beginning of NAM therapy in cases of preterm birth and apply a regular drinking plate until the correlated age of 1 week. Our results also showed that the resulting force at the age of 4 weeks and 3.5 months was less than the previously defined threshold value; this therefore allows regular NAM therapy until cheiloplasty at 3 months of age.

In contrast to other active treatment modalities, such as the Latham method with its bony fixation and screw for the activated expansion of the palate,<sup>50</sup> NAM represents a passive plate without active components. The main intention of NAM therapy is guided growth. Consequently, the resulting forces and stress distributions are expected to be much lower than those in active applications. On the basis of our results, no immediate adverse effects can be expected with regard to the development of the viscerocranium and neurocranium. The beneficial effect of improved alveolar and nasal symmetry and the potential reduction of secondary correction might outweigh possible adverse effects as reported by others.

As claimed earlier, long-term analyses of children treated with NAM and other presurgical modalities have to be conducted.<sup>51</sup> In particular, the incidence of suspected unwanted effects, such as retraction of the premaxilla, midfacial retrusion and the increased need for LeFort I osteotomies,<sup>13</sup> occlusal sequela, and the missing effectiveness compared with untreated infants therapy need to be analyzed in further, standardized studies with accurate evaluation of facial and alveolar growth.

### Limitations

FEA is only a close approximation to reality and is not able to analyze the in vivo situation. However, our presented results are valid, because the performed convergence analysis shows good consistency within the model. In this study, we have only examined the worst-case scenario with a high force being applied and without segmentation of the sutures. The absorption of force conduction is also not illustrated. Thus, the actual values of the von Mises stress distribution are expected to be even lower. The generation of realistic FE models of skulls of neonates is, however, generally difficult, because of the limited valid data regarding the E-modulus and the precise age-matched

material properties of bone, cartilage, and soft tissue of newborns and neonates.

## CONCLUSIONS

No adverse effects of NAM therapy on the development of the viscerocranium and neurocranium are to be expected when NAM is started later than the date of birth. In cases of preterm birth, initial treatment should be restricted to conventional feeding plates only until the corrected age.

**Lucas M. Ritschl, MD, DMD**

Department of Oral and Maxillofacial Surgery  
Klinikum rechts der Isar Technische Universität München  
Ismaningerstr. 22, D-81675 München, Germany  
E-mail: Lucas.Ritschl@tum.de

## ACKNOWLEDGMENTS

*All persons who have contributed to the study are listed as authors, because everyone has met the listed criteria for authorship.*

## REFERENCES

- Grayson BH, Santiago PE, Brecht LE, et al. Presurgical nasoalveolar molding in infants with cleft lip and palate. *Cleft Palate Craniofac J.* 1999;36:486–498.
- Rau A, Ritschl LM, Mücke T, et al. Nasoalveolar molding in cleft care—experience in 40 patients from a single centre in Germany. *PLoS One.* 2015;10:e0118103.
- Bennun RD, Perandones C, Sepiarsky VA, et al. Nonsurgical correction of nasal deformity in unilateral complete cleft lip: a 6-year follow-up. *Plast Reconstr Surg.* 1999;104:616–630.
- Garfinkle JS, King TW, Grayson BH, et al. A 12-year anthropometric evaluation of the nose in bilateral cleft lip-cleft palate patients following nasoalveolar molding and cutting bilateral cleft lip and nose reconstruction. *Plast Reconstr Surg.* 2011;127:1659–1667.
- Abbott MM, Meara JG. Nasoalveolar molding in cleft care: is it efficacious? *Plast Reconstr Surg.* 2012;130:659–666.
- Chang CS, Liao YF, Wallace CG, et al. Long-term comparison of the results of four techniques used for bilateral cleft nose repair: a single surgeon's experience. *Plast Reconstr Surg.* 2014;134:926e–936e.
- Patel PA, Rubin MS, Clouston S, et al. Comparative study of early secondary nasal revisions and costs in patients with clefts treated with and without nasoalveolar molding. *J Craniofac Surg.* 2015;26:1229–1233.
- Ritschl LM, Rau A, Güll FD, et al. Pitfalls and solutions in virtual design of nasoalveolar molding plates by using CAD/CAM technology—a preliminary clinical study. *J Craniomaxillofac Surg.* 2016;44:453–459.
- Gong X, Yu Q. Correction of maxillary deformity in infants with bilateral cleft lip and palate using computer-assisted design. *Oral Surg Oral Med Oral Pathol Oral Radiol.* 2012;114:S74–S78.
- Yu Q, Gong X, Shen G. CAD presurgical nasoalveolar molding effects on the maxillary morphology in infants with UCLP. *Oral Surg Oral Med Oral Pathol Oral Radiol.* 2013;116:418–426.
- Sischo L, Chan JW, Stein M, et al. Nasoalveolar molding: prevalence of cleft centers offering NAM and who seeks it. *Cleft Palate Craniofac J.* 2012;49:270–275.
- Niranjane PP, Kamble RH, Diagavane SP, et al. Current status of presurgical infant orthopaedic treatment for cleft lip and palate patients: a critical review. *Indian J Plast Surg.* 2014;47:293–302.
- Berkowitz S. The facial growth pattern and the amount of palatal bone deficiency relative to cleft size should be considered in treatment planning. *Plast Reconstr Surg Glob Open.* 2016;4:e705.



14. Vyas RM, Kim DC, Padwa BL, et al. Primary premaxillary setback and repair of bilateral complete cleft lip: indications, technique, and outcomes. *Cleft Palate Craniofac J.* 2016;53:302–308.
15. Berkowitz S. Response to the article “Primary Premaxillary Setback and Repair of Bilateral Complete Cleft Lip: Indications, Technique, and Outcomes”. *Cleft Palate Craniofac J.* 2017;54:493.
16. Voo K, Kumaresan S, Pintar FA, et al. Finite-element models of the human head. *Med Biol Eng Comput.* 1996;34:375–381.
17. Holberg C. Effects of rapid maxillary expansion on the cranial base—an FEM-analysis. *J Orofac Orthop.* 2005;66:54–66.
18. Huempfer-Hierl H, Schaller A, Hierl T. Biomechanical investigation of the supraorbital arch—a transient FEA study on the impact of physical blows. *Head Face Med.* 2014;10:13.
19. Huempfer-Hierl H, Bohne A, Wollny G, et al. Blunt forehead trauma and optic canal involvement: finite element analysis of anterior skull base and orbit on causes of vision impairment. *Br J Ophthalmol.* 2015;99:1430–1434.
20. Kumar A, Ghafoor H, Khanam A. A comparison of three-dimensional stress distribution and displacement of naso-maxillary complex on application of forces using quad-helix and nickel titanium palatal expander 2 (NPE2): a FEM study. *Prog Orthod.* 2016;17:17.
21. Nagasao T, Miyamoto J, Nagasao M, et al. The effect of striking angle on the buckling mechanism in blowout fracture. *Plast Reconstr Surg.* 2006;117:2373–2380; discussion 2381.
22. Schaller A, Voigt C, Huempfer-Hierl H, et al. Transient finite element analysis of a traumatic fracture of the zygomatic bone caused by a head collision. *Int J Oral Maxillofac Surg.* 2012;41:66–73.
23. Hammond AB, Smahel Z, Moss ML. Finite element method analysis of craniofacial morphology in unilateral cleft lip and palate prior to palatoplasty. *J Craniofac Genet Dev Biol.* 1993;13:47–56.
24. Işeri H, Tekkaya AE, Oztan O, et al. Biomechanical effects of rapid maxillary expansion on the craniofacial skeleton, studied by the finite element method. *Eur J Orthod.* 1998;20:347–356.
25. Sasaki A, Takeshita S, Publico AS, et al. Finite element growth analysis for the craniofacial skeleton in patients with cleft lip and palate. *Med Eng Phys.* 2004;26:109–118.
26. Bauer FX, Heinrich V, Grill FD, et al. Establishment of a finite element model of a neonate’s skull to evaluate the stress pattern distribution resulting during nasoalveolar molding therapy of cleft lip and palate patients. *J Craniofac Surg.* 2018;46:660–667.
27. McPherson GK, Kriewall TJ. The elastic modulus of fetal cranial bone: a first step towards an understanding of the biomechanics of fetal head molding. *J Biomech.* 1980;13:9–16.
28. Najarian SP. Infant cranial molding deformation and sleep position: implications for primary care. *J Pediatr Health Care.* 1999;13:173–177.
29. Steinberg JP, Rawlani R, Humphries LS, et al. Effectiveness of conservative therapy and helmet therapy for positional cranial deformation. *Plast Reconstr Surg.* 2015;135:833–842.
30. Nielsen BW, Mølsted K, Kjaer I. Maxillary and sella turcica morphology in newborns with cleft lip and palate. *Cleft Palate Craniofac J.* 2005;42:610–617.
31. Ehmman GW, Pfeifer G, Gundlach K. Morphological findings in unoperated cleft lips and palates. *Cleft Palate J.* 1976;13:262–272.
32. Uzel A, Alparslan ZN. Long-term effects of presurgical infant orthopedics in patients with cleft lip and palate: a systematic review. *Cleft Palate Craniofac J.* 2011;48:587–595.
33. Bongaarts CA, Kuijpers-Jagtman AM, van ‘t Hof MA, et al. The effect of infant orthopedics on the occlusion of the deciduous dentition in children with complete unilateral cleft lip and palate (Dutchcleft). *Cleft Palate Craniofac J.* 2004;41:633–641.
34. Bongaarts CA, van ‘t Hof MA, Prah-Andersen B, et al. Infant orthopedics has no effect on maxillary arch dimensions in the deciduous dentition of children with complete unilateral cleft lip and palate (Dutchcleft). *Cleft Palate Craniofac J.* 2006;43:665–672.
35. Bongaarts CA, Prah-Andersen B, Bronkhorst EM, et al. Infant orthopedics and facial growth in complete unilateral cleft lip and palate until six years of age (Dutchcleft). *Cleft Palate Craniofac J.* 2009;46:654–663.
36. Heidbuchel KL, Kuijpers-Jagtman AM, Freihofer HP. An orthodontic and cephalometric study on the results of the combined surgical-orthodontic approach of the protruded premaxilla in bilateral clefts. *J Craniofac Surg.* 1993;21:60–66.
37. Voshol IE, van der Wal KG, van Adrichem LN, et al. The frequency of Le Fort I osteotomy in cleft patients. *Cleft Palate Craniofac J.* 2012;49:160–166.
38. Heliövaara A, Leikola J, Hukka J. Craniofacial cephalometric morphology and later need for orthognathic surgery in 6-year-old children with bilateral cleft lip and palate. *Cleft Palate Craniofac J.* 2013;50:e35–e40.
39. Lee CT, Grayson BH, Cutting CB, et al. Prepubertal midface growth in unilateral cleft lip and palate following alveolar molding and gingivoperiosteoplasty. *Cleft Palate Craniofac J.* 2004;41:375–380.
40. Barillas I, Dec W, Warren SM, et al. Nasoalveolar molding improves long-term nasal symmetry in complete unilateral cleft lip-cleft palate patients. *Plast Reconstr Surg.* 2009;123:1002–1006.
41. Margulies SS, Thibault KL. Infant skull and suture properties: measurements and implications for mechanisms of pediatric brain injury. *J Biomech Eng.* 2000;122:364–371.
42. Coats B, Margulies SS. Material properties of human infant skull and suture at high rates. *J Neurotrauma.* 2006;23:1222–1232.
43. Roth S, Raul JS, Willinger R. Finite element modelling of paediatric head impact: global validation against experimental data. *Comput Methods Programs Biomed.* 2010;99:25–33.
44. Li Z, Hu J, Reed MP, et al. Development, validation, and application of a parametric pediatric head finite element model for impact simulations. *Ann Biomed Eng.* 2011;39:2984–2997.
45. Wolański W, Larysz D, Gzik M, et al. Modeling and biomechanical analysis of craniosynostosis correction with the use of finite element method. *Int J Numer Method Biomed Eng.* 2013;29:916–925.
46. Gačnik F, Ren Z, Hren NI. Modified bone density-dependent orthotropic material model of human mandibular bone. *Med Eng Phys.* 2014;36:1684–1692.
47. Jiang B, Zhu F, Cao L, et al. Computational study of fracture characteristics in infant skulls using a simplified finite element model. *J Forensic Sci.* 2017;62:39–49.
48. Li X, Sandler H, Kleiven S. The importance of nonlinear tissue modelling in finite element simulations of infant head impacts. *Biomech Model Mechanobiol.* 2017;16:823–840.
49. Chang CS, Wallace CG, Pai BC, et al. Comparison of two nasoalveolar molding techniques in unilateral complete cleft lip patients: a randomized, prospective, single-blind trial to compare nasal outcomes. *Plast Reconstr Surg.* 2014;134:275–282.
50. Latham RA, Kusy RP, Georgiade NG. An extraorally activated expansion appliance for cleft palate infants. *Cleft Palate J.* 1976;13:253–261.
51. van der Heijden P, Dijkstra PU, Stellingsma C, et al. Limited evidence for the effect of presurgical nasoalveolar molding in unilateral cleft on nasal symmetry: a call for unified research. *Plast Reconstr Surg.* 2013;131:62e–71e.